Proceedings of the 17th World Congress
The International Federation of Automatic Control
Seoul, Korea, July 6-11, 2008

Modeling and Control of Electrical Breakdown Process of Carbon Nanotubes ⋆

Yilun Luo * **Ning Xi** * **King Wai Chiu Lai** * **Hongzhi Chen** *
Jiangbo Zhang * **Lianqing Liu** *
T.J. Tarn **

* *Dept. of Electrical and Computer Engg., Michigan State University, East Lansing, MI 48824 USA (e-mail: xin@egr.msu.edu)*
** *Dept. of Systems Science and Math, Washington University, St. Louis, MO 63130 USA (e-mail: tarn@wuauto.wustl.edu)*

Abstract: Carbon nanotubes (CNTs) have been found as the promising semiconducting material for the future high performance nanoelectronics. As an important property for applications of a semiconductor, the band gap of a multi-walled CNT is related to its diameter. The capability of adjusting the material band gap is extremely important in sensor and electronics manufacturing. This paper discusses a real-time control method for the selective carbon shell breakdown process to tailor the CNT's band structure. The control method is designed based on the quantum state space model that describes the electron transport in the CNT. The state space anomaly during breakdown process can be observed using robust fault diagnosis technique by combining analytical approach and heuristic approach. The experimental results reported in this paper verify the theoretical findings. As a result, a MWCNT can be converted into a semiconducting material with pre-determined band gap.

Keywords: Quantum control, Nano and micro technologies, Fault diagnosis, and Fault detection.

1. INTRODUCTION

Carbon nanotubes (CNTs) are cylindrical fullerene molecules with nano-scale diameters (Dresselhaus et al. (1996)). The crystalline structure of a multi-walled CNT (MWCNT) can be considered as coaxial wrapping of multiple layers of graphite sheets into a cylinder, see Fig. 1.

Due to this unique crystalline structure and strong covalent carbon-carbon sp^2 bonding, semiconducting CNTs have outstanding electronic properties, such as 1-D near ballistic transport, lack of surface dangling bonds, and chemical robustness. These unique properties make CNT an excellent semiconductor over the conventional Si material for future high performance electronics. Much progress has been made in different applications, such as nanotransistors (Dai et al. (2006)), infrared detectors (Levitsky et al. (2003)), light emitting devices (Misewich et al. (2003)), logic circuits (Bachtold et al. (2001)), and chemical sensors (Valentini et al. (2003)).

Selecting of CNTs for particular electrical property remains a major challenge to turn the results of these theoretical studies to realistic devices. The synthesized CNTs are mixed in powder form with different band gaps. Due to the self-aggregation, nanoparticle measurement, manipulation and fabrication problems, it is difficult to choose a nanotubes according to the desired band structure for a specific application.

⋆ This research work is partially supported under NSF Grants IIS-0713346 and DMI-0500372, and ONR Grants N00014-04-1-0799 and N00014-07-1-0935.

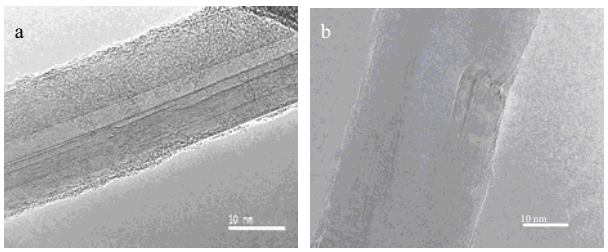

Fig. 1. The transmission electron microscopy (TEM) image of multi-walled carbon nanotubes.

Arnold et al. (2006) demonstrated a method using using sonication and centrifugation to separate and extract functionalized CNTs into different band gaps, which are roughly inverse proportional to their diameters. However, to prevent self-aggregation, the CNTs are treated by attaching functional groups to increase their solubility. The functionalization may degrade the excellent electrical property. This selection method still have difficulty to accurately obtain a nanotube with specific band structure and it is difficult to implement in a manufacturing process.

Instead of sorting and selecting for desired nanotube, Minot et al. (2003), proposed a on-chip bandgap engineering method. The CNT's band gap is capable to be altered by mechanically bending strain using the probe tip of the atomic force microscope (AFM). The P_Z surface bonds of CNT overlaps due to its geometrical deformation. But this structural transform may induce unstable defects, and is not feasible for batch fabrication.

The electrical breakdown process of MWCNT is proposed by Collins et al. (2001) to tailor the CNTs' band gaps. The carbon shells in a MWCNT can be electrically removed when applying current beyond the breakdown limits. A gate electrode under the CNTs is implemented to deplete the semiconducting shell for selectively protection, which enables efficiently converting a metallic device into a semiconductor one. However, this band structure engineering method remains uncontrolled which will result in cascade breakdown.

The bandgap of a semiconductor material is an important property for many applications, such as optical detectors, and solar cells. However, it has been one of the most challenging topics in semiconductor research to produce a material with a desired bandgap.

Recently, our experimental results have shown that the bandgap of a semiconducting MWCNT depends on the diameter of its outermost layer. If we can control the diameter of a multi-wall CNT, we can generate a semiconductor material with a prespecified bandgap. The basic idea is that we will start with a multi-walled CNT with relative large diameter and small bandgap. We will use a electrical breakdown process to remove the outer layer of the CNT. If we can precisely control the breakdown process, we will be able to produce a semiconducting CNT with a desired bandgap. The controller is designed based on a quantum electron transport model to generate the optimal electron transmission inside the nanotube for the breakdown process. An extended Kalman filter was used to estimate the system state, and detect the rapid change of the states caused by the electron movement in CNT. This kind of system fault usually represents the occupance of the electrical breakdown. Experiments verified that the breakdown process can be precisely controlled to remove the outer layers of a MWCNT.

2. QUANTUM ELECTRON TRANSPORT MODEL

The current-induced defect formation can cause the electrical breakdown of the CNT shells. After losing the outermost conducting carbon shell, the current transport property can be altered and tailored because of the band structure change. In order to control the breakdown current, it is important to investigate the current-voltage characteristics of a particular CNT.

The current transport of CNTs, as a semiconducting material, is composed of free electrons and holes in the conduction and valence bands. However, due to nano crystalline structure of CNT, the allowed energy levels in the conduction and valence bands are quantized. The classical transport model may neglect the quantum effects such as quantum tunneling, level broadening and wave function interference. A quantum transport model is derived based on non-equilibrium Green's functions (NEGF) and self-consistent electrostatistics for our breakdown device.

2.1 Non-Equilibrium Green's Functions

The NEGF method was developed by S. Datta (Datta. (2005)). This formulation can be used to solve Schrödinger's equation under non-equilibrium conditions and is capable

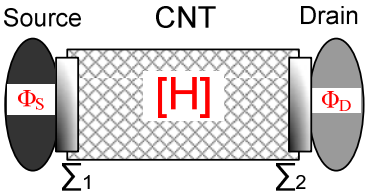

Fig. 2. The quantum model derived for the the electrical breakdown device. The electron transport inside a MWCNT is injected by source and drain electrodes with potential ϕ_S and ϕ_D.

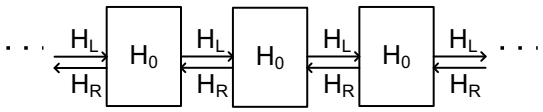

Fig. 3. The derivation of the Hamiltonian matrix for a given carbon nanotube.

of treating the contact coupling effect and dissipative scattering process in the channel.

In our electric breakdown experiment, a single MWCNT is bridged between two metal electrodes with small overlaps. The device can be modeled as shown in Fig. 2. The quantum energy states and electron wave function inside the CNT can be modeled by the Hamiltonian matrix H in (2), which is derived from Schrödinger's equation (1).

$$\left(-\frac{\hbar^2}{2m}\nabla^2 + U(\overrightarrow{r})\right)\Psi = E(\overrightarrow{r})\,\Psi \tag{1}$$

$$H\,\Psi = E\,\Psi \tag{2}$$

where Ψ is the wave function, $\hbar$ is the Dirac constant, m is the electron mass, $\overrightarrow{r}$ is the position vector and $U(\overrightarrow{r})$ is the potential energy.

A CNT is composed of unit carbon rings along the translational direction following its periodic lattice structure, seeing Fig. 3. Based on the Bloch's theory (Ashcroft et al. (1976)) and the tight binding approximation (Yang et al. (1999)), the Hamiltonian matrix for the whole CNT can be derived by the Hamiltonian matrix of the unit ring, H_0 in (3), and the left and right coupling from the neighboring units H_L and H_R. The Hamiltonian matrix H for a MWCNT, which is determined by its diameter, can be derived using the above method. Collins et al. (2001) experimentally verified that the electron transport is mainly contributed by the contacts of outermost carbon shell with the electrodes. The quantum tunneling between the carbon walls in the MWCNT can be neglected.

$$H = \begin{bmatrix} H_0 & H_R & 0 & & & \dots \\ H_L & H_0 & H_R & 0 & & \dots \\ 0 & H_L & H_0 & H_R & 0 & \dots \\ & 0 & H_L & H_0 & H_R & 0 \dots \\ & & & \dots & & \end{bmatrix} \tag{3}$$

Electrons with high electrochemical potential in the source attempt to occupy the empty quantum energy states in the CNT channel, while the drain, with low electrochemical potential, will keep pulling electrons out to establish equilibrium. Because of the coupling effect by the contact, the quantum states from the channel and metal will diffuse to the other material and the allowed quantum energy

levels are broadened. The self-energy matrix, Σ_S and Σ_D describe the electron flow through the contact between the metal electrodes and CNT.

The source-drain current can be derived as (4), which can be thought of as the difference of the electron transmission contributed from the source and drain.

$$I = \frac{4e}{h} \int T(E)[f_0(E - \phi_S) - f_0(E - \phi_D)]dE \qquad (4)$$

where e is the electron charge. h is the Planck constant. $\phi_{S(D)}$ is the electrostatic potential at the source(drain). f_0 is the Fermi-Dirac function, which represents the possibility of an electron to occupy an available quantum state in the channel. The transmission matrix $T(E)$ is defined by (5) below, which is proportional to the densities of states at given energy levels.

$$T(E) = \text{Trace}(\Gamma_S G \Gamma_D G^+) \qquad (5)$$

The Γ matrix represents energy level broadening due to electrode and CNT contact, see (6) below.

$$\Gamma_S = i(\Sigma_S - \Sigma_S^+),\ \Gamma_D = i(\Sigma_D - \Sigma_D^+), \qquad (6)$$

The retarded Green's function G matrix is derived for the lifetime of the quantum energy state and the broadening of the density of states (Datta. (2005)).

$$G(E) = [(E + i0^+)\,\mathrm{I} - H - \Sigma_S - \Sigma_D]^{-1} \qquad (7)$$

However, the derivation of the Hamiltonian matrix H requires the electrostatic potential $\phi(\overrightarrow{r})$ at each periodic carbon ring. The quantum state inside the nanotube channel will be affected by carrier propagation flux due to potential difference between the source and drain .

2.2 Poisson's Equation

The electrostatic potential ϕ of a CNT can be calculated by Poisson's equation.

$$\nabla^2 \phi(\overrightarrow{r}) = -\frac{e}{\varepsilon}\rho \qquad (8)$$

where e is the electron charge, ε is the dielectric constant and ρ is for the charge density .

By solving the NEGF formulas, the charge density ρ within the CNT channel can be derived as (9). $G^n(E)$ is the contact correlation function at energy E which causes inscattering into the channel (Datta. (2005)).

$$\rho = \int dE\, G^n(E)/2\,\pi \qquad (9)$$

2.3 Self Consistent Algorithm

The electron transport of the CNT device can be obtained by iteratively solving the the NEGF formulas and Poisson's equation. Each iteration will give an improved estimation for the next step. When the self-consistency is achieved, the numerical solution to the NEGF transport equation can be obtained, see Fig. 4.

The NEGF formulas and Poisson's equation for a specific device can be derived based on the 3-D information measured from an AFM. Experimental results demonstrate

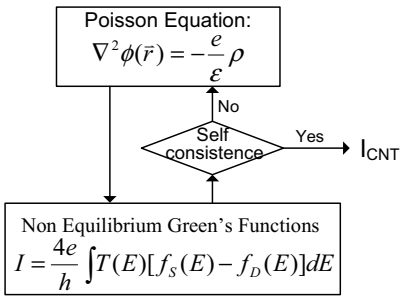

Fig. 4. Self consistence loop for the numerical calculation of the NEGF formulists and Poisson's equation.

that the electron transport in a MWCNT mainly happens in the outermost carbon shell (Collins et al. (2001)). We can calculate the Hamiltonian matrix H according to the diameter and channel length of the CNT. The self-energy matrix Σ for the nanotube contact can be obtained from the electrode size and contact length. For a given source-drain voltage, the current across the CNT can be evaluated using the self-consistence non-equilibrium Green's function formulas.

3. CARBON NANOTUBE ELECTRICAL BREAKDOWN CONTROLLER

An electron transmission model calculated from the self-consistence NEGF method, which gives the optimal estimation of the current-voltage characteristic of a specific device, is utilized as the state space model for breakdown current control.

The self-consistence algorithm for solving the electron transport model is computationally intensive. For a given voltage, it is difficult to calculate the current in real-time because of the huge size for the atom by atom Hamiltonian matrix, the self-consistence convergence for iteration, and matrix inversion difficulty when deriving the Green's function.

In order to calculate the numerical solution in real-time, the state space model is derived based on the optimal fitting by the effective-mass transport model (Tamura et al. (1998)) for the self-consistence result. Although the semiclassical model in (10) may lose accuracy for large drain voltage due to the simplification of quantum effect (Koswatta et al. (2004)), it follows the characteristic features of curvature, which is critical to estimate the breakdown voltage. After combing the NEGF result and effective-mass equation, the modeling error is tolerable for the breakdown application.

$$I_{CNT} = (4e/h)k_B T\{\ln[\frac{1 + \exp(\eta_{FS}/k_B T)}{1 + \exp(\eta_{FD}/k_B T)}]\} \qquad (10)$$

where $\eta_{F,S(D)} = \phi_{S(D)} - \phi_{barr}$, denotes the potential difference between the source(drain), $\phi_{S(D)}$ and the barrier height of the metal-semiconductor contact, ϕ_{barr}. I_{CNT} is the current in the CNT device. T is the temperature in kelvin. And k_B is the Boltzmann constant. In experiment, the the source is grounded and ϕ_S equals to zero. And ϕ_{barr} can be calculated by the optimal fitting from the NEGF result. Thus, I_{CNT} is completely determined by the drain voltage ϕ_D.

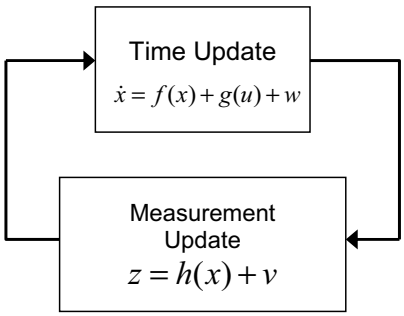

Fig. 5. The recursive iteration for an Extended Kalman filter: Time Update and Measurement Update.

3.1 Extended Kalman filter for Fault Detection

The quantum current controller design is base on an extended Kalman filter. The extended Kalman filter is a real-time nonlinear recursive algorithm to estimate the state of a dynamic system from discrete and noisy measurements. It is least-square optimal based on maximum a posterior probability (MAP) (Kalman. (1960)).

The iterative process of the extended Kalman filter includes two steps. The time update step projects the current system state and its statistical information forward in time according to system plant. The measurement update step adjusts the propagated estimate by an actual measurement based on statistical decision theory and the least-square method. Fig. 5 demonstrates the ongoing extended Kalman filtering loop.

The controller is developed as follows. The system state, x, is defined using the potential difference between the source and drain, U_{SD}. The polynomial quantum electron transport model, $h_p(x)$, is integrated in the measurement update stage. During the electrical breakdown process, the voltage across the CNT electrodes is increased by steps, u. Thus, in continuous time form, the extended Kalman filter loop can be derived as (11) and (12).

$$\dot{x} = u \tag{11}$$

$$z = h_p(x) \tag{12}$$

For real-time control, the discrete extended Kalman filter is derived according to the above dynamic system. The time update of the extended Kalman filter is obtained as (13) and (14).

$$\hat{x}_k^- = \hat{x}_{k-1} + u_k \tag{13}$$

$$P_k^- = P_{k-1} + Q \tag{14}$$

where $\hat{x}$ is the system state for the source drain potential difference generated by the controller. The control variable u_k is the potential change in each iteration step. P is the error covariance matrix . Q is the covariance of the modeling error.

The measurement update of the extended Kalman filter can be obtained as (15), (16) and (17).

$$K_k = P_k^- H^T (H P_k^- H^T + R)^{-1} \tag{15}$$

$$\hat{x}_k = \hat{x}_k^- + K_k(z_k - H\hat{x}_k^-) \tag{16}$$

$$P_k = (I - K_k H) P_k^- \tag{17}$$

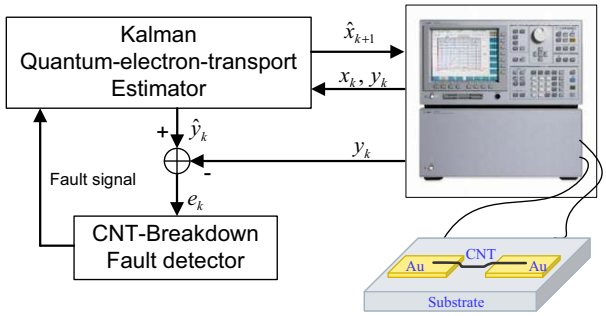

Fig. 6. The CNT electrical breakdown system for on-chip bandgap engineering.

where K is the Kalman gain, R is the measurement noise covariance, z is the measurement of the current flow through the CNT device, and H is the observation matrix, which is the Jacobean matrix derived from the quantum electron transport model, see (18).

$$H = \left.\frac{\partial h_p}{\partial x}\right|_{\hat{x}_{k-1}, u_k} = -\frac{4q\ \exp(\zeta_{DB})}{h\{\exp(1+\zeta_{DB})\}} \tag{18}$$

$$\zeta_{DB} = \hat{x}_k^- - \phi_{barr} \tag{19}$$

Thus the system state for the control voltage is optimally propagated based on the statistical information from the previous data, while the incoming current measurement of the CNT is utilized to adjust the projected estimation. The Gaussian random noise in modeling and measurement is filtered during iteration.

The rapid change of the electron movement in the CNT can be detected as the system fault in the quantum transport controller by exploring the analytical redundancy information of the system space (Frank. (1990)). Based on a robust parameter estimation approach, the fault observer is modeled by generating the Mahalanobis distance, see (20). The breakdown voltage is stopped immediately once r exceeds a fault threshold to prevent cascade breakdown.

$$r = (z_k - H\hat{x}_k^-)^T P_k^{-1} (z_k - H\hat{x}_k^-) \tag{20}$$

4. EXPERIMENTAL RESULTS

Extensive experiments are performed to test the performance of the control algorithm and the system design. The system structure of the CNT bandgap control system is demonstrated in Fig. 6. The Kalman estimator and fault detector algorithm are implemented in computer by controlling the Agilent's 4156C Precision Semiconductor Parameter Analyzer to generate the optimal breakdown voltage signal based on the current through the CNT as feedback. The $2\,\mu V/1\,fA$ high resolution output, 50 KHz high sampling rate of the 4156C analyzer, and the high speed computer-analyzer communication are capable to guarantee the real-time and high-precision control.

The MWCNTs are of nanoscale in diameter and normally 3-5 μm in length. Thus micro chips with electrode pairs are fabricated using photolithography process to make electrical connections. The gold electrodes were designed with small gap distance of 1-2 μm, so as to connect one single tube. The MWCNTs powder was dissolved in the acetone and dispersed by ultrasonication for 10-15 minutes to form CNT suspension. After pipet deposition onto the

Fig. 7. A microelectronic device fabricated by a single MWCNT using DEP deposition and nanomanipulation.

microchip, the CNT in the suspension is attracted by the dielectrophoretic (DEP) force generated from the micro electrode pair until bridged across it. The amplitude, frequency of the DEP signal, and the solution concentration are experimentally optimized to maximize the possibility to trap a single nanotube between the electrodes (Lai et al. (2007)). The AFM based automanipulation system developed in our lab (Li et al. (2004)) is implemented to clean up the impurity particles and extra nanotubes, and also to adjust for better contact and sensitivity area. As a result, an individual MWCNT can be deposited to the micro electrode pair with optimal contacts as illustrated in Fig. 7.

Fig. 8 below demonstrates the experimental results for the control process of electrical breakdown. In order to pill off the outer carbon shell and prevent cascade breakdown, the breakdown voltage was increased according to the optimal estimate from the extended Kalman filter, which is designed based on the quantum electron transport model. Utilizing the statistical information of the current data as feedback, the modeling error and random measurement noise are least mean-square optimally minimized by the filter but not losing the quick response to the current change in the the voltage estimation. As shown in the figure, the controller is capable to generate stable breakdown voltage even when the current become noisy and unstable when approaching the breakdown. And the controller decreased the voltage immediately following with the current drop to prevent the cascade breakdown. The random current jitters caused by measurement noise will not yield large fault residual to affect the fault decision and cause a false alarm. The fault threshold is experimentally optimized to minimize the false alarm and maintain quick response. Because the electrical breakdown is independent of the voltage increasing rate, the controller is designed to keep constant breakdown voltage for a short period during each iteration step to increase accuracy and sampling rate, and therefore reduce the probability of cascade breakdown. The abrupt current change from 98.683 μA to 93.224 μA, was observed when the control voltage was increased to 1.996 volts. The control voltage is immediately switched off in order to stop the breakdown process.

Fig. 9 illustrates the AFM scan images and cross section height data of the MWCNT during the breakdown experiments. After the outer carbon shells were electrically pilled off, the diameter of the MWCNT was reduced from 197.991 nm to 118.07 nm. The inner carbon shell with smaller di-

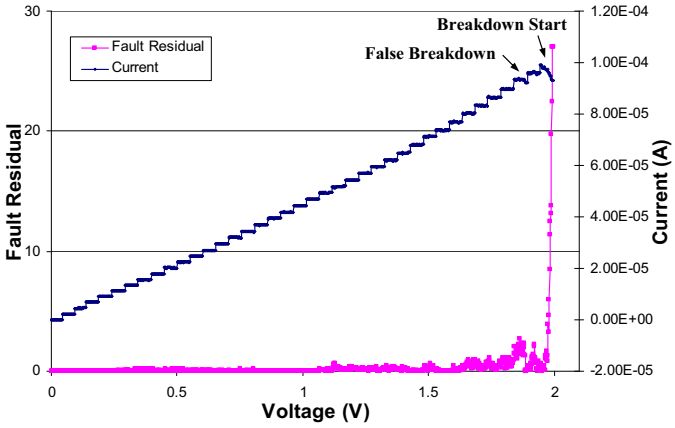

Fig. 8. Experimental result of the real-time control of CNT breakdown. The current change caused by the carbon shell breakdown can be immediately detected.

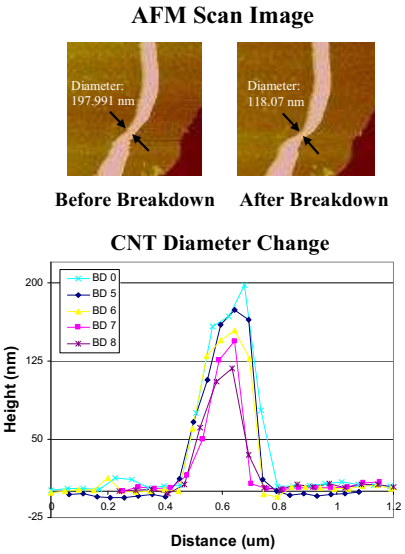

Fig. 9. The AFM image indicating CNT diameter was reduced after break control process.

ameter became the new contributor to electron transport. Because the bandgap of CNT is inversely related to its diameter, the conductivity is reduced and the MWCNT's material characteristic is altered and become more semiconducting. As demonstrated in Fig. 10, the MWCNT was tailored from a metallic material to a semiconductor after the sixth breakdown and become semiconducting with bigger band gaps.

5. CONCLUSIONS

A quantum electron transport controller based on quantum state model and the extended Kalman filter is developed for real-time CNTs electrical breakdown control. The controller is capable to filter the random noise in modeling and measurement as a minimum mean-square estimator (MMSE). Optimal breakdown electron transport through the CNT is generated by the controller based on the statistic information of the previous data. The controller is sensitive to the recent abnormal observation. Thus, false alarm can be prevented caused by random noise and big

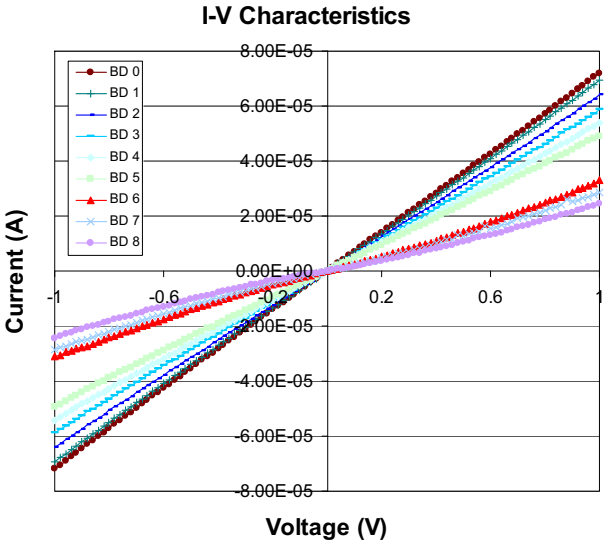

Fig. 10. Experimental results to demonstrate the performance of the quantum bandgap engineering controller.

electron transport change which is usually the occupance of breakdown can be detected immediately.

CNTs as a nano material has the advantages of quantum effects, low thermal noise, and ballistic transport. However, due to its nano size, it is difficult to fabricate or select CNTs with specific electrical property. Our breakdown control method, which is capable to adjust its band structure, provides a steady and high-yield on-chip band gap engineering approach in batch electronics fabrication process. This is especially important for CNTFET. It can also be used to adjust the sensing range of the optical or chemical sensor by tailoring the bandgap.

REFERENCES

M.S. Dresselhaus, G. Dresselhaus, and P.C. Eklund. *Science of Rullerenes and Carbon Nanotubes.* Academic Press, San Diego, 1996.

H.J. Dai, A. Javey, E. Pop, D. Mann and Y.R. Lu (2006). Electrical Transport Properties and Field-Effect Transistors of Carbon Nanotubes. *Nano: Brief Reports and Reviews*, volume 1, pages 1–4.

I.A. Levitsky, and W.B. Euler (2003). Photoconductivity of Single-walled Carbon Nanotubes under CW illumination. *Appl. Phys. Lett.*, volume 83, pages 1857–1859.

J.A. Misewich, R. Martel, P. Avouris, J.C. Sang, S. Heinze, and J. Tersoff (2003). Electrically induced optical emission from a carbon nanotube FET. *Science*, volume 300, pages 783–786.

A. Bachtold, P. Hadley, T. Nakanishi and C. Dekker (2001). Logic circuits with carbon nanotube transistors. *Science*, volume 294, pages 1317–1320.

L. Valentini, I. Armentano, J.M. Kenny, C. Cantanini, L. Lozzi, and S. Satucci (2003). Sensors for sub-ppm NO2 gas detection based on carbon nanotube thin films. *Appl. Phys. Lett.*, volume 82, pages 4623.

M.S. Arnold, A.A. Green, J.F. Hulvat, S.I. Stupp, and M.C. Hersam (2006). Sorting carbon nanotubes by electronic structure using density differentiation. *Nature nanotechnology*, volume 1, pages 60–65.

E.D. Minot, Y. Yaish, V. Sazonava, J.Y. Park, M. Brink, and P.L. McEuen (2003). Tuning Carbon Nanotube Band Gaps with Strain. *Physical Review Letters*, volume 90, pages 156401.

P.G. Collins, M.S. Arnold, and P. Avouris (2001). Engineering Carbon Nanotubes and Nanotube Circuits Using Electrical Breakdown. *Science*, volume 292, pages 706–709.

S. Datta. *Quantum Transport: Atom to Transistor.* Cambridge University Press, New York, 2005.

N.W. Ashcroft, and D. Mermin. *Solid State Physics.* Holt, Reinhart and Winston, New York, 1976.

L. Yang, M.P. Anantram, J. Han, and J.P. Lu (1999). Effect of small uniaxial and torsional strain. *Physical Review B*, volume 60, pages 13874–13878.

R. Tamura, and M. Tsukada (1998). Analysis of Quantum Conductance of Carbon Nanotube Junctions by the Effective-mass Approximations. *Phys. Rev. B*, volume 58, pages 8120–8124 (1998).

S. Koswatta, N. Neophytou, D. Kienle, G. Fiori, and M. Lundstrom (2006). Dependence of DC Characteristics of CNT MOSFETs on Bandstructure Models. *IEEE Trans. on Nanotechnology*, volume 5, pages 368–372 (2006).

R.E. Kalman (1960). A New Approach to Linear Filtering and Prediction Problems. *Transactions of the ASME - Journal of Basic Engineering*, volume 82, pages 35–45 (1960).

P.M. Frank (1990). Fault diagnosis in dynamic systems using analytical and knowledge-based redundancy – a survey and some new results. *Automatica*, volume 26, pages 459–474 (1990).

W.C. Lai, N. Xi, and U.C. Wejinya (2007). Automated process for manufacturing carbon nanotube (CNT) based nano devices. *Proceedings of the 7th IEEE International Conference on Nanotechnology*, pages 474–479, August 2007.

G. Li, N. Xi, and M. Yu (2004). Development of augmented reality system for AFM based nanomanipulation. *IEEE/ASME Trans. on Mechatronics*, volume 9, pages 358–365 (2004).